A Conformational and Structure−Activity Relationship Study of Cytotoxic 3,5-Bis(arylidene)-4-piperidones and Related *N*-Acryloyl Analogues

Jonathan R. Dimmock,*[,†] Maniyan P. Padmanilayam,[†] Ramanan N. Puthucode,[†] Adil J. Nazarali,[†] Narasimhan L. Motaganahalli,[†] Gordon A. Zello,[†] J. Wilson Quail,[‡] Eliud O. Oloo,[‡] Heinz-Bernhard Kraatz,[‡] Jared S. Prisciak,[§] Theresa M. Allen,[⊥] Cheryl L. Santos,[⊥] Jan Balzarini,[∥] Erik De Clercq,[∥] and Elias K. Manavathu[△]

Departments of Chemistry and Biochemistry, College of Pharmacy and Nutrition, University of Saskatchewan, Saskatoon, Saskatchewan, S7N 5C9 Canada, Department of Pharmacology, University of Alberta, Edmonton, Alberta, T6G 2H7 Canada, Rega Institute for Medical Research, Katholieke Universiteit Leuven, B-3000 Leuven, Belgium, and Department of Medicine, Wayne State University, Detroit, Michigan 48201-1908

Received June 16, 2000

A series of 3,5-bis(arylidene)-4-piperidones **1** and related *N*-acryloyl analogues **2** were prepared as candidate cytotoxic agents with a view to discerning those structural features which contributed to bioactivity. A number of the compounds were markedly cytotoxic toward murine P388 and L1210 leukemic cells and also to human Molt 4/C8 and CEM neoplasms. Approximately 40% of the IC_{50} values generated were lower than the figures obtained for melphalan. In virtually all cases, the *N*-acyl compounds were significantly more bioactive than the analogues **1**. In general, structure−activity relationships revealed that the cytotoxicity of series **1** was correlated positively with the size of the aryl substituents, while in series **2**, a $-\sigma$ relationship was established. In particular, various angles and interatomic distances were obtained by molecular modeling, and the presence of an acryloyl group on the piperidyl nitrogen atom in series **2** affected the relative locations of the two aryl rings. This observation, along with some differences in distances between various atoms in series **1** and **2**, may have contributed to the disparity in cytotoxicity between **1** and **2**. The results obtained by X-ray crystallography of representative compounds were mainly in accordance with the observations noted by molecular modeling. Selected compounds interfered with the biosynthesis of DNA, RNA, and protein in murine L1210 cells, while others were shown to cause apoptosis in the human Jurkat leukemic cell line. This study has revealed the potential of these molecules for development as cytotoxic and anticancer agents.

Introduction

A number of α,β-unsaturated ketones display cytotoxic and anticancer properties.[1,2] The rationale for their synthesis and antineoplastic evaluation is based in part on their predicted mode of action, i.e., interaction with cellular thiols with little or no affinity for hydroxy and amino groups found in nucleic acids.[3,4] Thus development of these compounds as candidate cytotoxics may lead to drugs which are bereft of the genotoxic properties present in certain antineoplastic agents.[5] Conversion of certain conjugated enones into the corresponding Mannich bases led to significant increases in both the rates of thiol alkylation[6] and cytotoxicity.[7] The increased rate of thiolation may be due to the protonated Mannich bases stabilizing the reaction intermediates formed between thiols and the α,β-unsaturated keto group to a significantly greater extent than occurs with the precursor enones.

A number of tumors have lower pH than corresponding normal cells.[8] Hence Mannich bases may display selective toxicity to such neoplasms since there will be a higher percentage of the molecules in the ionized form in the tumors (and hence present as the more reactive species) than is the case with the corresponding α,β-unsaturated ketones. Such considerations led to the decision a number of years ago to prepare **1a** which may be considered a Mannich base of a dienone. This compound showed high activity toward the murine lymphocytic leukemia P388/MRI cell line and did not bind to a synthetic DNA, poly [d(AT)].[9] Acyclic Mannich bases of conjugated styryl ketones generally caused mortality when administered to mice using doses of 200 mg/kg or more.[7,10] However, five consecutive daily doses of 240 mg/kg of **1a** did not induce fatalities.[9] The compound therefore is markedly cytotoxic but has low murine toxicity. Thus the preparation of a number of analogues of **1a** was planned. To discern whether there was a correlation between the electronic and/or hydrophobic properties of the aryl substituents and cytotoxicity, groups with divergent Hammett σ and Hansch π values were placed in the aryl rings. In fact, substituents from three of the four quadrants of a Craig plot[11] were utilized.

There was, however, a further reason for the preparation of series **1**. The theory of sequential cytotoxicity

* Corresponding author. Address: College of Pharmacy and Nutrition, University of Saskatchewan, 110 Science Place, Thorvaldson Building, Room 216, Saskatoon, Saskatchewan, S7N 5C9 Canada. Phone: (306) 966-6331. Fax: (306) 966-6377. E-mail: dimmock@skyway.usask.ca.
† College of Pharmacy and Nutrition, University of Saskatchewan.
‡ Department of Chemistry, University of Saskatchewan.
§ Department of Biochemistry, University of Saskatchewan.
⊥ University of Alberta.
∥ Katholieke Universiteit Leuven.
△ Wayne State University.

10.1021/jm0002580 CCC: $20.00
Published on Web 01/20/2001

Scheme 1. Syntheses of Series **1** and **2**[a]

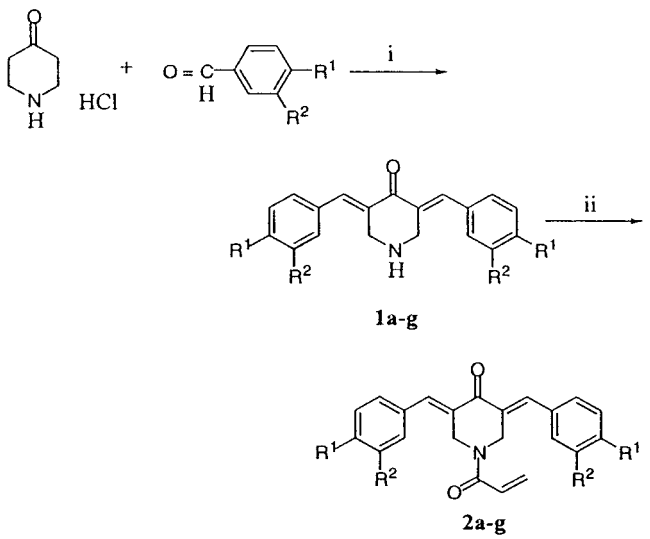

[a] Reagents: (i) HCl/CH_3COOH followed by treatment with K_2CO_3; (ii) CH_2=CHCOCl/K_2CO_3. The letters **a**−**g** indicate the following substituent pattern: **a**: $R^1 = R^2 = H$; **b**: R^1 = Cl, R^2 = H; **c**: $R^1 = R^2$ = Cl; **d**: R^1 = F, R^2 = H; **e**: $R^1 = NO_2$, R^2 = H; **f**: $R^1 = OCH_3$, R^2 = H; **g**: $R^1 = N(CH_2)_2$, R^2 = H.

states that successive chemical attacks may lead to greater damage in cancer cells compared to normal cells.[12] The evidence marshalled to support this viewpoint has been presented at length.[12] Thus, in the case of the compounds in series **1**, initial reaction with a thiol such as glutathione would lead to the formation of the corresponding 3-arylglutathionylmethyl-5-arylidene-4-piperidone which is capable of further reaction with cellular nucleophiles, i.e., one would predict successive reactions in vitro and in vivo. To evaluate the hypothesis further, the formation of the *N*-acryloyl analogues **2** was considered. In these molecules, an additional site for electrophilic attack of biomacromolecules is present. If the hypothesis of sequential cytotoxicity is valid, the compounds in series **2** should be appreciably more cytotoxic than the corresponding secondary amines **1**. The objective of the present investigation therefore was to prepare two series of prototypic molecules **1** and **2** with a view to discerning the structural features contributing to cytotoxicity and to examining further the viability of the theory of sequential cytotoxicity.

Results and Discussion

The compounds in series **1** and **2** were prepared by a procedure outlined in Scheme 1. A Claisen−Schmidt condensation between 4-piperidone hydrochloride and the appropriate aryl aldehyde led to the formation of the 3,5-bis(arylidene)-4-piperidones **1**. Acylation of these enones with acryloyl chloride gave rise to the corresponding *N*-acyl derivatives **2**. ^{1}H NMR spectroscopy revealed the presence of a single peak for the methine protons adjacent to the aryl rings, indicating the stereohomogeneity of these molecules. Since X-ray crystallography of **1b**,**e** and **2b**,**d** (vide infra) revealed these molecules to possess the *E* configuration, which is consistent with previous reports for this cluster of compounds,[9] the assumption was made that all members of series **1** and **2** had the *E* stereochemistry.

The 4-piperidones in series **1** and **2** were examined against murine P388 and L1210 neoplasms since these cell lines have been claimed to be predictors of clinically useful anticancer drugs.[13] In addition, evaluation using human Molt 4/C8 and CEM T-lymphocytes was undertaken in order to ascertain whether the compounds were cytotoxic to human neoplastic cells. Cytotoxicity was undertaken using concentrations of compounds up to and including 50 μM in the case of the P388 screen and 500 μM for the remaining cell lines. The results are summarized in Table 1.

In general, the compounds displayed marked cytotoxicity toward the cell lines. However, the IC_{50} figures for **2g** in the L1210 and CEM screens were not obtained, and clearly this compound is an outlier with markedly lower activity than the analogues **2a**−**f**. Consequently, further discussion pertaining to structure−activity relationships will revolve around **2a**−**f** and the analogues in series **1**, namely **1a**−**f**. The average IC_{50} figures for **1a**−**f** in the P388, L1210, Molt 4/C8, and CEM screens were 0.81, 81.9, 59.4, and 33.6 μM, respectively, while the comparable figures for **2a**−**f** were 0.28, 4.71, 0.96, and 1.13 μM, respectively. These data reveal that P388 cells are the most sensitive to these compounds in contrast to L1210 cells which are the most refractory. The huge differential in the activity of these compounds toward the two murine cell lines may be due, in part at least, to the fact that P388 cells grow far more slowly than L1210 cells. The results for **1a**−**f** and **2a**−**f** reveal that 44% of the IC_{50} figures presented in Table 1 were lower than melphalan, revealing the importance of these compounds as prototypic molecules from which further development should take place. The average IC_{50} figures for all four cell lines for **1a**−**f** and **2a**−**f** were 44.0 and 1.77 μM, respectively, revealing a 25-fold increase in cytotoxicity for the *N*-acryloyl analogues which affords support for the theory of sequential cytotoxicity. To obtain an overview of the cytotoxicity of the compounds, average potency (AP) figures derived from all four cell lines were calculated. Since these data were derived from different cell lines of both murine and human origin, they should be viewed with caution; nevertheless they enable one to observe rapidly the relative cytotoxicity of different compounds. These figures are presented in Table 1.

To discern whether correlations existed between the Hammett σ, Hansch π, and molecular refractivity (MR) figures of the aryl substituents and cytotoxicity, the decision was made to construct linear and semilogarithmic plots between these physicochemical constants and the IC_{50} values of **1a**−**f** and **2a**−**f** against each of the four cell lines as well as the AP figures. These types of regression analyses have been used by us previously.[2] Logarithmic transformations were performed on the data in an attempt to stabilize the variances and to linearize the relationships. The correlations were classified as highly significant ($p < 0.05$), significant ($p < 0.1$), or as a trend toward a significant correlation ($p < 0.15$). In the case of compounds **1a**−**f**, semilogarithmic plots revealed the following relationships in which the *p* values were less than 0.15, namely between the IC_{50} values and the aryl σ figures for the P388 cells ($p < 0.15$) and also between the MR constants using L1210 cells ($p < 0.1$), Molt 4/C8 cells ($p < 0.15$), and CEM cells ($p < 0.15$) as well as the AP values ($p < 0.15$). Both linear and semilogarithmic plots between the cytotoxicity of

Table 1. Cytotoxicity of **1a**−**g** and **2a**−**g** against Murine P388 and L1210 Cells and Also Human Molt 4/C8 and CEM T-Lymphocytes

	IC_{50} (μM)				
compd	P388 cells	L1210 cells	Molt 4/C8 cells	CEM cells	AP[a]
1a	0.77 ± 0.02	7.96 ± 0.11	1.67 ± 0.15	1.70 ± 0.02	3.03
1b	0.74 ± 0.07	41.5 ± 0.3	13.4 ± 4.0	8.63 ± 0.48	16.1
1c	1.01 ± 0.06	129 ± 80	40.2 ± 1.3	20.8 ± 16.0	47.8
1d	0.60 ± 0.01	36.2 ± 0.1	5.00 ± 1.20	2.05 ± 0.36	11.0
1e	0.20 ± 0.01	32.9 ± 4.2	8.28 ± 0.75	4.47 ± 2.28	11.5
1f	1.54 ± 0.3	244 ± 43	288 ± 8	164 ± 104	174
1g	0.64 ± 0.06	240 ± 92	226 ± 18	162 ± 19	157
2a	0.50 ± 0.06	8.69 ± 0.73	1.42 ± 0.27	1.48 ± 0.34	3.30
2b	0.15 ± 0.02	1.96 ± 0.08	0.44 ± 0.06	0.49 ± 0.23	0.76
2c	0.05 ± 0.007	1.52 ± 0.02	1.04 ± 0.76	1.08 ± 0.82	0.92
2d	0.27 ± 0.01	3.89 ± 0.18	0.41 ± 0.24	0.80 ± 0.46	1.34
2e	0.05 ± 0.001	0.42 ± 0.07	0.15 ± 0.06	0.26 ± 0.02	0.22
2f	0.68 ± 0.05	11.8 ± 0.7	2.27 ± 0.17	2.67 ± 0.32	4.36
2g	43.29 ± 3.5	>500	369 ± 185	>500	>353
melphalan	0.22 ± 0.01	2.13 ± 0.02	3.24 ± 0.56	2.47 ± 0.21	2.02

[a] Average potency of all four cell lines.

2a−**f** and the Hammett σ values revealed the following results: P388 cells, $p < 0.05$; L1210 cells, $p < 0.05$; Molt 4/C8 cells, $p < 0.15$; CEM cells, ($p < 0.1$); AP values, $p < 0.05$. In all of these plots, the r values were negative when σ values were employed and positive when the MR constants were considered. All other plots led to p values in excess of 0.15.

The following conclusions may be drawn from the structure−activity relationships (SAR) study. First, in the case of the *N*-acyl analogues **2a**−**f**, electronic parameters are clearly the most important factor influencing cytotoxicity. Thus future expansion of series **2** should bear in mind this correlation. These results are similar to a recent study with cytotoxic 2-arylidenebenzosuberones wherein cytotoxicity was negatively correlated with the aryl σ values using P388 and L1210 cells and positively correlated with the MR constants in all of the same four cell lines employed in this report.[2] However, the negative correlation between cytotoxicity and the Hammett σ values was counterintuitive since one would predict that, by decreasing the fractional positive charge on the arylidene methine carbon atom, cytotoxicity would decrease rather than be elevated. Thus interaction with cellular thiols may not be the predominant mechanism mediating toxicity. Second, the lipophilicity of the molecules appears to exert little or no influence on the antineoplastic activity of the compounds **1a**−**f** and **2a**−**f**.

In addition to evaluating the contributions of the aryl substituents to bioactivity, the topology of the molecules was considered. This segment of the work was undertaken principally to determine those structural features which contribute to the marked disparity in cytotoxicity between the compounds in series **1** and **2**. The shapes of **1a**−**g** and **2a**−**g** were generated by molecular modeling, and the measurements obtained are illustrated in Figures 1−3. The torsion angles θ_1 and θ_2 were formed between rings A and B and the adjacent olefinic linkages, respectively, while the width and length of the molecules were reflected in the d_1 and d_2 measurements, respectively. To obtain the relative positions of the aryl rings, the distances d_3 between the centers of the rings were determined. Axis 1 was the plane in which ring A was located. The plane of ring B was noted, and the distances d_4 and angles ψ between the two planes were

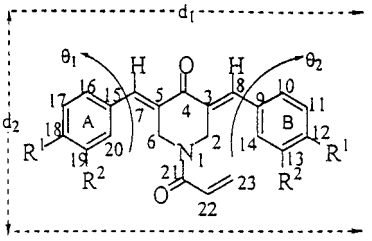

Figure 1. Numbering of the compounds in series **1** and **2** and designation of the θ_1 and θ_2 torsion angles and interatomic distances d_1 and d_2.

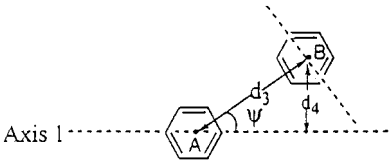

Figure 2. Indication of the interatomic distances d_3 and d_4 and angle ψ.

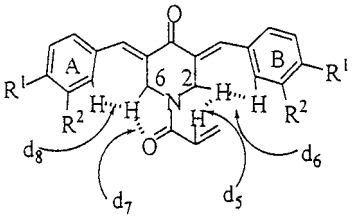

Figure 3. Denotation of the interatomic distances d_5−d_8.

obtained. The results of these determinations are summarized in Table 2.

The percentage increases in the torsion angles θ_1 and θ_2 in series **2**, compared to the analogues in series **1**, were 8 and 24, respectively. Thus a contributing factor for the greater cytotoxicity of the *N*-acyl analogues may be the elevated θ_2 figures and to a less extent the θ_1 values found in **2**. The orientations of the aryl rings in **2** may permit more favorable alignments of the rings with a critical biomacromolecule; for example, a better fit into a cleft on a bonding site may occur in the compounds **2** than is the case with series **1**.

The data in Table 2 revealed that the distances d_1−d_3 in series **1** and **2** were similar; the greatest disparity of 9% was noted in the case of the d_2 values. It is possible therefore that the lengths of the molecules may

Table 2. Certain Angles and Distances of Compounds **1a**−**g** and **2a**−**g** Determined by Molecular Modeling

	angles (deg)			interatomic distances (Å)							
compd	θ_1	θ_2	ψ	d_1	d_2	d_3	d_4	d_5	d_6	d_7	d_8
1a−**g**	−49.5 ± 0.05	49.4 ± 0.11	37.0 ± 0.08	16.80 ± 2.78	5.03 ± 0.70	10.23 ± 0.004	3.25 ± 0.01		2.39 ± 0.005		2.39 ± 0.005
2a−**g**	−53.2 ± 0.17	61.0 ± 0.24	97.3 ± 0.24	16.68 ± 2.83	5.47 ± 0.26	10.22 ± 0.005	3.73 ± 0.09	2.15 ± 0.005	2.44 ± 0.012	2.42 ± 0.001	2.48 ± 0.014

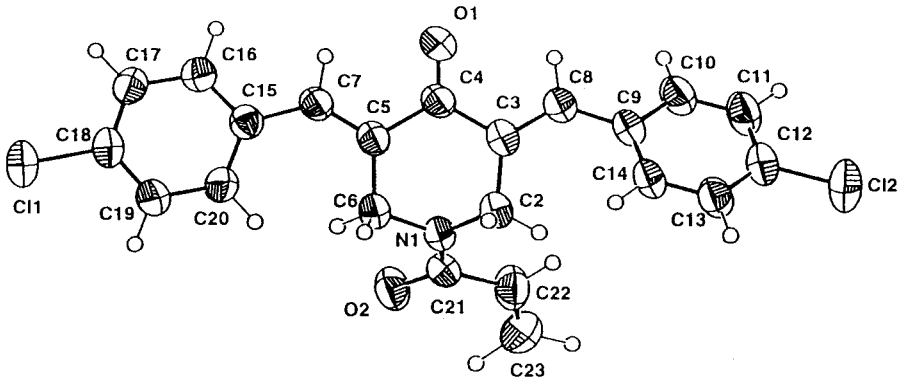

Figure 4. ORTEP diagram of **2b**.

Table 3. Some Torsion Angles and Distances of **1e** and **2b**,**d** Determined by X-ray Crystallography[a]

	angles (deg)			interatomic distances (Å)								
compd	θ_1	θ_2	ψ	d_1	d_2	d_3	d_4	d_5	d_6	d_7	d_8	AP
1b	18.6	−15.6	7.91	16.46	5.73	10.08	1.39		2.14		2.16	16.1
	(−49.5)	(49.4)	(36.99)	(15.92)	(4.99)	(10.23)	(3.25)		(2.39)		(2.39)	
1e	19.6	−23.0	1.59	17.44	4.62	10.32	0.29		2.28		2.18	11.5
	(−49.5)	(49.4)	(36.96)	(17.15)	(4.64)	(10.23)	(3.24)		(2.39)		(2.39)	
2b	11.4	−27.9	6.21	16.42	6.13	10.36	1.13	1.91	2.14	2.29	2.11	0.76
	(61.3)	(53.2)	(97.59)	(15.88)	(5.38)	(10.21)	(3.65)	(2.15)	(2.44)	(2.42)	(2.48)	
2d	20.0	−19.3	0.83	15.63	7.49	10.34	0.15	1.89	2.17	2.26	2.11	1.34
	(−53.2)	(−61.1)	(97.43)	(15.17)	(5.39)	(10.22)	(3.81)	(2.16)	(2.44)	(2.43)	(2.48)	

[a] Figures in parentheses were obtained by molecular modeling.

make only a minor contribution to the variation in cytotoxicity between **1** and **2**. On the other hand, ring B in series **2** was located further away from axis 1 as revealed by a 15% increase in the d_4 figures in the *N*-acyl compounds. This observation was further illustrated in the 163% increase in the ψ figures of series **2** compared to the analogues in series **1**.

The distances d_5−d_8 were measured with a view to explaining the differences between the θ_1, θ_2, ψ, and d_4 figures of the piperidones **1** and the corresponding amides **2**. The d_5 and d_7 values in series **2** will indicate whether nonbonded interactions between the vinyl proton and oxygen atom, attached to carbon atoms 22 and 21, respectively, interact with the equatorial protons at positions 2 and 6 of the piperidine ring. Second, the d_6 and d_8 distances may reveal whether steric impedance occurs between the ortho protons of the aryl rings and the 2 H^e and 6 H^e atoms. In general, an interatomic distance between the centers of two atoms which is 2.5 Å or less is an indication of a nonbonded interaction. If the increased figures of θ_1, θ_2, ψ, and d_4 in series **2** were due to nonbonded interactions, as indicated in Figure 3, then the interatomic distances d_5 and d_6 would be predicted to be shorter than d_7 and d_8, respectively, i.e., $d_5 < d_7$ in series **2** and $d_6 < d_8$ in both series **1** and **2**. The figures in Table 2 reveal that only the first postulate was validated, i.e., $d_5 < d_7$, and thus additional factors account for the differences in orientation and location of rings A and B.

One may summarize the molecular modeling data by stating that the acyl group attached to the N1 atom in series **2** has a significant effect on the spatial orientation and location of aryl ring B which may well contribute markedly to the greater cytotoxicity of series **2** compared to series **1**. Thus expansion of series **2**, in which groups of varying sizes are attached to the N1 atom, may shed further light on the structural features contributing to the cytotoxicity in this novel series of candidate antineoplastic agents.

X-ray crystallography was undertaken on representative compounds in series **1** and **2** with a view to discerning whether the observations pertaining to the shapes of compounds **1** and **2**, determined by molecular modeling, were corroborated or not using a second physicochemical approach. Data were obtained for **1b** and **1e**,which crystallized in the protonated form with three molecules of acetic acid, and **2b**,**d**. An ORTEP diagram of **2b** is portrayed in Figure 4. In all four compounds the *E* configuration of the chiral axes was revealed, and the piperidine ring assumed the half chair conformation.

A review of the data in Table 3 led to the following observations. First, the θ_1 and θ_2 angles, although smaller than those recorded using molecular modeling, confirmed the lack of coplanarity of the rings A and B with the adjacent dienone structure. In general, the $\theta_2 > \theta_1$ relationship was noted. Second, in the crystal state, however, the aryl rings were virtually in the same plane

Table 4. Peak Potentials of **1a**−**d**,**f**,**g** and **2b**,**d**,**g**

compd	E_p (mV)[a]	compd	E_p (mV)[a]	compd	E_p (mV)[a]
1a	1208	**1d**	1323	**2b**	1134
1b	1230	**1f**	1270	**2d**	1180
1c	1345	**1g**	1064	**2g**	970

[a] A scan rate of 100 mV s^{-1} was used.

Table 5. Inhibitory Effects of **1e**,**g** and **2e** on the Biosyntheses of DNA, RNA, and Protein in Murine L1210 Cells

	IC_{50} (μM)			
compd	DNA	RNA	protein	L1210 cells
1e	228	276	214	32.9
1g	≥500	336	320	240
2e	2.77	5.73	3.21	0.42
melphalan	>100	>100	94.6	2.13

as revealed by the small ψ and d_4 figures. Third, the d_5−d_8 measurements revealed extensive nonbonded interactions. In concert with the molecular modeling data, the distance d_5 was shorter than d_7 while the d_6 and d_8 measurements were virtually identical. Therefore, in general, the evidence of X-ray crystallography on selected molecules was in accord with the topological studies conducted by molecular modeling.

A correlation has been established previously between the cytotoxicity of various conjugated enones and their redox potentials.[14] In the present investigation, attempts were made to measure this physicochemical parameter of all of the compounds in series **1** and **2**. However, oxidation of **2a**,**c**,**e** was not achieved, and the scans for **1e** and **2f** in the region of 1500 and 1700 mV, respectively, were extremely broad and definitive oxidation potentials could not be ascertained. All other systems exhibited an irreversible one electron oxidation at a scan speed of 100 mV s^{-1}. The results for the remaining compounds are presented in Table 4. Both linear and semilogarithmic plots between the E_p figures of **1a**−**d**,**f**,**g** and the Hammett σ values showed positive correlations ($p < 0.05$). However, no relationships were noted between the redox potentials of these compounds and the IC_{50} figures using either the four cell lines or the AP figures ($p > 0.15$). Thus the cytotoxicity of the compounds in series **1** was not related to their redox potentials. In the case of **2b**,**d**,**g**, there was no correlation between the E_p and σ values ($p > 0.15$). Since **2g** has markedly divergent activity against the four cell lines than the analogues and hence eliminated from further consideration, there was an insufficient number of compounds in series **2** to evaluate whether the cytotoxicity of these compounds correlated with their redox potentials.

An initial investigation into the possible manner whereby these compounds exerted their cytotoxicity was undertaken with special reference to discerning why such a marked disparity in bioactivity was noted between the compounds in series **1** and **2**. A number of anticancer drugs inhibit the biosyntheses of DNA, RNA, and proteins.[15] The data in Table 5 indicate the far greater inhibitory effect of **2e** on macromolecular syntheses than **1e**. In fact, the average IC_{50} figures against DNA, RNA, and protein syntheses of **1e** and **2e** are 239 and 3.90 μM, respectively, indicating that **2e** is 61 times more potent than **1e**. These results may partially explain the 78-fold greater activity of **2e** toward L1210 cells than **1e**. In addition, the greater cytotoxicity of **1e** than that of **1g** to L1210 cells was reflected in the lower IC_{50} values of **1e** toward DNA, RNA, and protein syntheses. The data in Table 5 reveal that the useful lead molecule **2e** acts in a different way to the established anticancer drug melphalan whose principal mode of action is direct interaction with DNA[16] and, from the results portrayed in Table 5, apparently does not interfere markedly with the syntheses of DNA, RNA, and proteins.

Table 6. Cytotoxicity, Apoptotic Indices, and Inhibition of RNA and Protein Biosynthesis of **1c** and **2c** Using Human Jurkat T Cells

compd	IC_{50} (μM)	IC_{80} (μM)	apoptotic index[a]	% inhibition of synthesis of RNA[a]	% inhibition of synthesis of protein[a]
1c	3.09	4.83	48.3	26.4 ± 9.48	31.1 ± 6.09
2c	0.58	0.94	63.5	67.6 ± 1.55	58.1 ± 4.52
melphalan	2.20[b]	3.52[b]	63.2[b]	85.1[b] ± 4.71	17.3 ± 4.94

[a] IC_{80} concentrations were used in these determinations. [b] Reprinted in part from *J. Med. Chem.* **1999**, *42*, 1363. Copyright 1999 American Chemical Society.

A number of anticancer drugs induce apoptosis,[17] and the question posed was whether representative compounds in series **1** and **2** acted by this mechanism. A previous study revealed that human Jurkat T cells were more sensitive to an α,β-unsaturated ketone than other cell lines,[18] and thus this neoplasm was employed in the present investigation. The data in Table 6 revealed that both **1c** and **2c** were cytotoxic to this cell line. To ensure that death occurred in the majority of cells, IC_{80} figures were generated, and using these concentrations both **1c** and **2c** caused apoptosis. The apoptotic index [(number of cells with apoptotic nuclei/number of cells counted) × 100] of **2c** was only 32% higher than **1c**, indicating that additional factors accounted for the 5-fold greater cytotoxicity of **2c** over **1c** toward Jurkat cells. In concert with the results recorded in Table 5, both **1c** and **2c** inhibited RNA and protein syntheses and greater activity was displayed by **2c**.

The results from the investigations of representative compounds summarized in Tables 5 and 6 revealed that these molecules inhibit macromolecular syntheses and caused apoptosis. In addition, the compounds in series **2** were more potent in causing these effects than the analogues in series **1**, affording some indication of the reasons for the greater cytotoxicity of the *N*-acyl congeners. One may speculate from these biodata that there are multiple sites of action of the 4-piperidones. If alkylation is the predominant cause of cytotoxicity, then of relevance is the fact that alkylating agents employed in cancer chemotherapy also have multiple sites of action.[19]

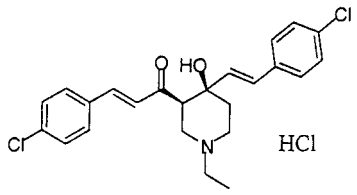

3

Recently the 1,3,4-trisubstituted piperidine **3** prepared in our laboratory was discovered to display activity toward a wide range of pathogenic fungi,

including a large number of isolates of *Aspergillus fumigatus* and *Candida albicans*.[20] Compound **3**, which contains a piperidine ring and two substituted styryl groups, one of which is conjugated to a carbonyl function, resembles the structures of the molecules in series **1** and **2**. Since there is an urgent need for novel antifungal agents different in structures and modes of action from currently available medication, representative compounds in series **1** and **2** were evaluated against three isolates of *Aspergillus fumigatus* and one isolate of *Candida albicans*. The average minimum inhibitory concentration (MIC) figures for **3** and an investigational azole voriconazole were 3.9 and 1.95 μM, respectively. However the MIC values of **1b**,**c**,**e** and **2b**,**c**,**e** were all above 500 μM in the four assays. Thus in reference to the screening procedures used in this investigation, the compounds displayed significant cytotoxicity toward both murine and human neoplasms yet were virtually bereft of antifungal activity. It is conceivable therefore that the compounds in series **1** and **2** are not general biocidal agents but target malignant cells, although a great deal of further study is required in order to evaluate the extent that these compounds display toxicity to cancers.

Conclusions

Many of the compounds prepared in this study were shown to demonstrate pronounced cytotoxicity toward four different tumor cell lines. *N*-Acryloylation of the secondary amino group in series **1** leading to the congeners **2** was clearly an important molecular change leading to a significant increase in bioactivity. This result is in accord with the theory of sequential cytotoxicity. Development of series **2** should take into consideration the -σ relationship established by the SAR investigations pertaining to the aryl substituents. Furthermore, altering the size of the substituent at position 1 may lead to considerable variations in the relative locations of the aryl rings which in turn may correlate with changes in cytotoxicity. These molecules have the potential for development into even more potent bioactive agents, and **2e**, possessing approximately nine times the potency of melphalan, is a particularly promising lead molecule. In addition, a number of questions have been raised in this study that may be addressed in subsequent investigations using this cluster of compounds. For example, experimentation could be undertaken with a view to discerning why cytotoxicity was influenced by the shapes of the molecules as well as identifying the biochemical mechanisms which cause these compounds to be pro-apoptotic agents.

Finally, recent studies have revealed the promising in vivo activities of both an α,β-unsaturated ketone[21] and a Mannich base of an enone,[22] thereby confirming the value of vigorously investigating these compounds.

Experimental Section

A. Chemistry. Melting points are uncorrected. Compounds **1c,g** and **2a,c** have been reported in the literature and, in general, had melting points similar to those recorded previously.[9,23] Elemental analyses (C, H, N) were undertaken by Mr. K. Thoms, Department of Chemistry, University of Saskatchewan, and are within 0.4% of the calculated values. ^{1}H NMR spectra were recorded for **1a**−**g** and **2a**−**g** using a Brucker AM 500 FT NMR machine (500 MHz). A Nonius CAD-4 diffractometer was used for the collection of X-ray crystallographic data. TLC was undertaken using silica gel plastic-backed sheets and a solvent system of 2% methanol in chloroform. Compounds **2e** and **2g** were obtained with 0.5 and 0.25 molecules of water of crystallization, respectively.

Synthesis of Series 1. The appropriate aryl aldehyde (26.71 mmol) was added to a suspension of 4-piperidone hydrochloride monohydrate (13.03 mmol) in acetic acid (35 mL). Dry hydrogen chloride was passed through this mixture for 0.5 h during which time a clear solution was obtained. After stirring at room temperature for 24 h, the precipitate was collected and added to a mixture of a saturated aqueous potassium carbonate solution (25% w/v, 25 mL) and acetone (25 mL); the resultant mixture was stirred for 0.5 h. The free base was collected, washed with water (50 mL), and dried. The compounds were recrystallized from 95% ethanol (**1a**,**e**), methanol (**1b**−**d**,**f**), or dimethylformamide (**1g**). The melting points (°C) and yields (%) of **1a**−**g** were as follows: **1a**: 177−178, 87; **1b**: 201, 82; **1c**: 196−197, 84; **1d**: 212−213, 75; **1e**: 205−206, 68; **1f**: 210−211, 100; **1g**: 238−240, 72. The ^{1}H NMR spectrum (DMSO-d_6) of a representative compound **1a** was as follows: δ 4.21−4.28 (s, 4H, piperidyl H), 7.42−7.52 (m, 10H, aryl H), 7.74 (s, 2H, arylidene H). The NH absorptions were not observed for most of the compounds in series **1**.

Synthesis of Series 2. Acryloyl chloride (8.84 mmol) was added to a suspension of the appropriate 3,5-bis(arylidene)-4-piperidone (5.75 mmol), acetone (10 mL), and a solution of potassium carbonate (29 mmol) in water (10 mL) which was cooled externally with an ice bath. After being stirred at room temperature for 12 h, the mixture was diluted with water (20 mL), and the precipitate was collected, washed with water (20 mL), dried, and recrystallized from 95% ethanol (**2a**−**f**) or dimethylformamide (**2g**). The melting points (°C) and yields (%) of **2a**−**g** were as follows: **2a**: 126−127, 79; **2b**: 154−156, 90; **2c**: 151, 78; **2d**: 213, 85: **2e**: 169−170, 68; **2f**: 180−182, 80; **2g**: 234, 58. The ^{1}H NMR spectrum ($CDCl_3$) of a representative compound **2d** was as follows: δ 4.70−4.82 (br s, 2H, piperidyl H), 4.82−4.96 (br s, 2H, piperidyl H), 5.60−5.65 (dd, 1H, J = 12.34 Hz, COC*H*=CH_2), 6.15−6.25 (m, 2H, COCH=C*H*$_2$), 7.10−7.20 (t, 4H, 3,5-aryl H), 7.32−7.50 (br s, 4H, 2,6-aryl H), 7.80 (s, 2H, arylidene H).

Structure−Activity Relationships. The σ, π, and MR values were taken from the literature.[24] Since the MR value of hydrogen is 1.03 and not 0.00, the sizes of the groups in both the 3- and 4-positions of the aryl rings were calculated. For example, in the case of **1a** and **2a**, the MR figure employed was 2.06 (2 × 1.03) while for the 4-chloro analogues **1b** and **2b** the MR value chosen was 7.06, i.e., 6.03 + 1.03 for the chloro and hydrogen atoms, respectively. In this way, differences in the sizes of the substituents were obtained. The statistical analysis was undertaken using commercial software.[25]

Molecular Modeling. Models were built using a MacroModel 4.5 program[26,27] which was followed by a conformational search using the Monte Carlo method and an amber force field to obtain the shapes of the compounds possessing minimal energy. The distances and angles in Tables 2 and 3 were obtained directly from the models using standard analytical geometrical procedures.

X-ray Crystallography of 1e and 2b,d. The compounds were recrystallized from benzene by slow evaporation (**1b**), ethanol−2-propanol by vapor diffusion (**1e**), ethanol by slow evaporation (**2b**), or methanol−2-propanol by vapor diffusion (**2d**). Compound **1e** crystallized as a trisolvate of acetic acid. Two of the three acetic acid molecules were involved in hydrogen bonding with N1. A Nonius CAD-4 diffractometer with a ω scan was used for data collection, and the structures were solved using NRCVAX[28] and refined using SHELXL97.[29] Atomic scattering factors were taken from the literature.[30] All non-hydrogen atoms were found on the E-map and refined anisotropically. Hydrogen atom positions were calculated and not refined.

Redox Potential Determinations. The electrochemical experiments were carried out using solutions of the compounds

(0.1 mM) in freshly distilled acetone which had been dried over anhydrous sodium sulfate. The supporting electrolyte was tetrabutylammonium perchlorate (0.1 M). Determinations were made using a Bioanalytical Systems Inc. (BAS) glassy carbon working electrode (diameter of 2 mm) and a platinum wire counter electrode. The reference electrode was a BAS silver/silver chloride electrode. A scan rate of 100 mV s^{-1} was employed. IR compensation was applied, and background scans of the supporting electrolyte were collected and subtracted from the spectra.

Biological Evaluations. The cytotoxic evaluation of the compounds in series **1** and **2** against P388D1 cells was undertaken using a literature procedure,[31] while the evaluation using murine L1210 cells as well as human Molt 4/C8 and CEM cells was carried out by a previously reported methodology.[32] Measurement of the inhibition of DNA, RNA, and protein syntheses in murine L1210 cells by selected compounds was accomplished using tritiated thymidine, uridine, and leucine, respectively. The cytotoxicity and apoptotic indices of **1c** and **2c** and melphalan using human Jurkat T cells was undertaken by a literature procedure[18] except that nigrosin dye was used instead of trypan blue in the cytotoxicity experiments and a solution of ethidium bromide (0.1% w/v) and acridine orange (0.1% w/v) was employed in measuring apoptosis. The inhibition of RNA and protein syntheses using tritiated uridine and ^{35}S-methionine, respectively, was measured by a literature procedure.[33] The antifungal evaluation of **1b**,**c**,**e** and **2b**,**c**,**e**,**3** and voriconazole was accomplished by a broth microdilution method described previously[20] using three isolates of *Aspergillus fumigatus* (ATCC 208995, ATCC 208996, ATCC 208967) and one of *Candida albicans* (ATCC 90028).

Acknowledgment. The authors thank the following agencies for financial support of the work described in this study (initials of investigator funded in parentheses): CoCensys Inc. (J.R.D.), the Natural Sciences and Engineering Research Council of Canada (A.J.N., J.W.Q., H.-B.K.), the National Cancer Institute of Canada (T.M.A.), and the Fonds voor Wetenschappelijk Onderzoek-Vlaanderen (J.B., E.D.C.). Dr. L. Prasad is thanked for her assistance in the execution and interpretation of the molecular modeling and X-ray crystallography experiments. Thanks are also extended to Mrs. C. Jamont who typed various drafts of the manuscript.

Supporting Information Available: Crystal data, atomic coordinates, equivalent isotropic displacement parameters, bond lengths and angles, anisotropic displacement parameters, hydrogen coordinates, isotropic displacement parameters, torsion angles, and ORTEP diagrams[34] for **1e**, **2b**,**d** as well as elemental analysis data for **1a**−**g**, **2a**−**2g**. This information is available free of charge via the Internet at http://pubs.acs.org.

References

(1) Dimmock, J. R.; Elias, D. W.; Beazely, M. A.; Kandepu, N. M. Bioactivities of chalcones. *Curr. Med. Chem.* **1999**, *6*, 1125−1149.
(2) Dimmock, J. R.; Kandepu, N. M.; Nazarali, A. J.; Kowalchuk, T. P.; Motaganahalli, N.; Quail, J. W.; Mykytiuk, P. A.; Audette, G. F.; Prasad, L.; Perjési, P.; Allen, T. M.; Santos, C. L.; Szydlowski, J.; De Clercq, E.; Balzarini, J. Conformational and quantitative structure−activity relationship study of cytotoxic 2-arylidenebenzocycloalkanones. *J. Med. Chem.* **1999**, *42*, 1358−1366.
(3) Mutus, B.; Wagner, J. D.; Talpas, C. J.; Dimmock, J. R.; Phillips, O. A.; Reid, R. S. 1-*p*-Chlorophenyl-4,4-dimethyl-5-diethylamino-1-penten-3-one hydrobromide, a sulfhydryl-specific compound which reacts irreversibly with protein thiols but reversibly with small molecular weight thiols. *Anal. Biochem.* **1989**, *177*, 237−243.
(4) Baluja, G.; Municio, A. M.; Vega, S. Reactivity of some α,*β*-unsaturated ketones towards sulfhydryl compounds and their antifungal activity. *Chem. Ind.* **1964**, 2053−2054.
(5) Benvenuto, J. A.; Connor, T. A.; Monteith, D. K.; Laidlaw, J. W.; Adams, S. C.; Matney, T. S.; Theiss, J. C. Degradation and inactivation of antitumor drugs. *J. Pharm. Sci.* **1993**, *82*, 988−991.
(6) Dimmock, J. R.; Smith, L. M.; Smith, P. J. The reaction of some nuclear substituted acyclic conjugated styryl ketones and related Mannich bases with ethanethiol. *Can. J. Chem.* **1980**, *58*, 984−991.
(7) Dimmock, J. R.; Taylor, W. G. Evaluation of nuclear-substituted styryl ketones and related compounds for antitumor and cytotoxic properties. *J. Pharm. Sci* **1975**, *64*, 241−249.
(8) Wike-Hooley, J. L.; van den Berg, A. P.; van der Zee, J.; Reinhold: H. S. Human tumour pH and its variation. *Eur. J. Cancer Clin. Oncol.* **1985**, *21*, 785−791.
(9) Dimmock, J. R.; Arora, V. K.; Wonko, S. L.; Hamon, N. W.; Quail, J. W.; Jia, Z.; Warrington, R. C.; Fang, W. D.; Lee, J. S. 3,5-bis-Benzylidene-4-piperidones and related compounds with high activity towards P388 leukemia cells. *Drug Des. Delivery* **1990**, *6*, 183−194.
(10) Dimmock, J. R.; Patil, S. A.; Leek, D. M.; Warrington, R. C.; Fang, W. D. Evaluation of acrylophenones and related bis-Mannich bases against murine P388 leukemia. *Eur. J. Med. Chem.* **1987**, *22*, 545−551.
(11) Craig, P. N. Interdependence between physical parameters and selection of substituent groups for correlation studies. *J. Med. Chem.* **1971**, *14*, 680−684.
(12) Dimmock, J. R.; Sidhu, K. K.; Chen, M.; Reid, R. S.; Allen, T. M.; Kao, G. Y.; Truitt, G. A. Evaluation of some Mannich bases of cycloalkanones and related compound for cytotoxic activity. *Eur. J. Med. Chem.* **1993**, *28*, 313−322.
(13) Suffness, M.; Douros, J. In *Methods in Cancer Research, Volume XVI, Part A*; De Vita, V. T., Jr., Busch, H., Eds; Academic Press: New York, 1979; p 84.
(14) Dimmock, J. R.; Kandepu, N. M.; Hetherington, M.; Quail, J. W.; Pugazhenthi, U.; Sudom, A. M.; Chamankhah, M.; Rose, P.; Pass, E.; Allen, T. M.; Halleran, S.; Szydlowski, J.; Mutus, B.; Tannous, M.; Manavathu, E. K.; Myers, T. G.; De Clercq, E.; Balzarini, J. Cytotoxic activities of Mannich bases of chalcones and related compounds. *J. Med. Chem.* **1998**, *41*, 1014−1026.
(15) Foye, W. O.; Sengupta, S. K. Cancer chemotherapy. In *Principles of Medicinal Chemistry*, 4th ed.; Foye, W. O., Lemke, T. L., Williams, D. A., Eds.; Williams and Wilkins: Media, PA, 1995; p 829.
(16) Silverman, R. B. *The Organic Chemistry of Drug Design and Drug Action*, Academic Press: San Diego, CA, 1992; pp 247−248.
(17) Tsurusawa, M.; Saeki, K.; Fujimoto, T. Differential induction of apoptosis on human lymphoblastic leukemia Nalm-6 and Molt-4 cells by various antitumor drugs. *Int. J. Hematol.* **1997**, *66*, 79−88.
(18) Vashishtha, S. C.; Nazarali, A. J.; Dimmock, J. R. Application of fluorescence microscopy to measure apoptosis in Jurkat T cells after treatment with a new investigational anticancer agent (NC 1213). *Cell. Mol. Neurobiol.* **1998**, *18*, 437−445.
(19) Patrick, G. L. *An Introduction to Medicinal Chemistry*; Oxford University Press: Oxford, 1995; p 74.
(20) Manavathu, E. K.; Vashishtha, S. C.; Alangaden, G. J.; Dimmock, J. R. In vitro antifungal activity of some Mannich bases of conjugated styryl ketones. *Can. J. Microbiol.* **1998**, *44*, 74−79.
(21) McMorris, T. C.; Yu, J.; Ngo, H.-T.; Wang, H.; Kelner, M. J. Preparation and biological activity of amino acid and peptide conjugates of antitumor hydroxymethylacyfulvene. *J. Med. Chem.* **2000**, *43*, 3577−3580.
(22) Dimmock, J. R.; Vashishtha, S. C., Patil, S. A.; Udupa, N.; Dinesh, S. B.; Devi, P. U.; Kamath, R. Cytotoxic and anticancer activities of some 1-aryl-2-dimethylaminomethyl-2-propen-1-one hydrochlorides. *Pharmazie* **1998**, *53*, 702−706.
(23) Dimmock, J. R.; Arora, V. K.; Duffy, M. J.; Reid, R. S.; Allen, T. M.; Kao, G. Y. Evaluation of some *N*-acyl analogues of 3, 5-bis-(arylidene)-4-piperidones for cytotoxic activity. *Drug Des. Discovery.* **1992**, *8*, 291−299.
(24) Hansch, C.; Leo, A. J. *Substituent Constants for Correlation Analysis in Chemistry and Biology*; John Wiley and Sons: New York, 1979; p 49.
(25) Statistical Package for the Social Sciences, SPSS for Windows, Standard Version, Release 9.0.0; SPSS Inc.: Chicago, IL, 1998.
(26) MacroModel, Version 4.5; Department of Chemistry, Columbia University: New York, August 1994.
(27) Mohamadi, F.; Richards, N. G. J.; Guide, W. C.; Liskamp, M.; Caufield, C.; Chang, G.; Hendrickson, T.; Still, W. C. MacroModel − An integrated software system for modeling organic and bioorganic molecules using molecular mechanics. *J. Comput. Chem.* **1990**, *11*, 440−467.

(28) Gabe, E. J.; LePage, Y.; Charland, J. P.; Lee, F. L.; White, P. S. An interactive program system for structure analyses. *J. Appl. Crystallogr.* **1989**, *22*, 384−387.
(29) Sheldrick, G. M. SHELXL-97. Program for the Refinement of Crystal Structures; University of Gottingen: Germany, 1997.
(30) *International Tables for X-ray crystallography*; Kynoch Press: Birmingham, 1974; Vol. IV.
(31) Phillips, O. A.; Nelson, L. A.; Knaus, E. E.; Allen, T. M.; Fathi-Afshar, R. Synthesis and cytotoxic activity of pyridylthio, pyridylsulfinyl and pyridosulfonyl methyl acrylates. *Drug Des. Delivery* **1989**, *4*, 121−127.
(32) Balzarini, J.; De Clercq, E.; Mertes, M. P.; Shugar, D.; Torrence, P. F. 5-Substituted 2-deoxyuridines; correlation between inhibition of tumor cell growth and inhibition of thymidine kinase and thymidylate synthetase. *Biochem. Pharmacol.* **1982**, *31*, 3673−3682.
(33) Martin, S. J.; Lennon, S. V.; Bonham, A. M.; Cotter, T. G. Induction of apoptosis (programmed cell death) in human leukemic HL-60 cells by inhibition of RNA and protein synthesis. *J. Immunol.* **1990**, *145*, 1859−1867.
(34) Johnson, C. K. *ORTEP II. Report ORNL − 5138*; Oak Ridge National Laboratory: Tennesse, 1976.

JM0002580